We are a platform for pharmacy experts to share high-quality research on drug discovery, pharmacology and related topics.

Featured Articles

Antibacterial plants from Gayo Lues Highland

January 9, 2023

Read More

Dear colleague,

You are cordially invited to submit a manuscript to the **Journal of Pharmacy & Pharmacognosy Research (JPPRes)** (ISSN 0719-4250), an international, bimonthly specialized and peer-reviewed open access journal devoted to the publication of original contributions in relevant areas, which publishes original research articles, reviews, letters and guest edited single topic issues in all areas of Pharmacy and Pharmacognosy in English or Spanish.

Papers of JPPRes are opening accessible at the journal's homepage: jppres.com, and you are invited to read or download them freely for the academic exchanges.

The Audience of JPPRes could be: Biochemists, Biotechnologists, Botanists, Chemical Engineers, Clinical Pharmacologists, Medical Scientists, Medicinal Chemists, Natural Product Chemists, Pharmaceutical Scientists, Pharmacologists, Pathologists, Plant Scientists, and Toxicologists, among others.

Frequency of publication: Electronic versions of articles are published immediately and continuously once the manuscripts have been accepted. JPPRes has an acceptance rate of 33.6% (2022). The average time between submission and final decision is 100 days and the average time between acceptance and final publication is 15 days. JPPRes does not charge any fee for authors submitting manuscripts. However, an article-processing charge **(APC) of 600 USD (US Dollars)** applies to papers accepted after peer review.

You are welcome to submit your manuscript to this journa through the following link: submit article

Please, visit the Author Guidelines, Submit an Article or contact us if you have any questions about the journal.

Best regards,

Prof. Gabino Garrido
Editor in Chief
E-mail

Indexed In:

Clarivate Master Journal List

JIF (2025): 1.0

2025 Journal Citation Reports™ (Clarivate, 2026)

CiteScore: 2.5 (2025)

(Scopus, 2026)

Google Scholar

Google Scholar

Journal of Pharmacy and Pharmacognosy Research

Q3 Complementary and Alternative Medicine

best quartile

SJR 2025 0.27

powered by scimagojr.com

Latest Articles

Antibacterial plants from Gayo Lues Highland

January 9, 2023

Read More

Targeted proteins for vaginal epithelial repair

January 2, 2023

Read More

Bioadsorption of silver ions by chitin derivatives

January 2, 2023

Read More

1 2 3 ... 67

Current Issue:

Volume 14, Issue 4

Volume 14, Issue 3

Recently Published Issues by Year:

2026 2025 2024 2023

2022 2021 2019 2018

2017 2016 2015 2014

2013

Issue In Progress:

Volume 14, Issue 5

© 2013-2020 by the authors; licensee JPPRes, Antofagasta, Chile. This journal is an open-access journal distributed under the terms and conditions of the Creative Commons Attribution license-Non Commercial 4.0 international. The content on this site is intended for health professionals. If you are not a health professional, please talk to your doctor about any doubts or concerns regarding your health

Site Update: October 25th, 2026

Made with ♥ by AVAGAX Studio

JPPRes | Journal of Pharmacy & Pharmacognosy Research

Archive

2026

Vol. 14

Volume 14, *Issue 6* (November-December), 2026

Volume 14, *Issue 5* (September-October), 2026

Volume 14, *Issue 4* (July-August), 2026

Volume 14, *Issue 3* (May-June), 2026

Volume 14, *Issue 2* (March-April), 2026

Volume 14, *Issue 1* (January-February), 2026

2025

Vol. 13

Volume 13, *Issue 6* (November-December), 2025

Volume 13, *Issue 5* (September-October), 2025

Volume 13, *Issue 4* (July-August), 2025

Volume 13, *Issue 3* (May-June), 2025

Volume 13, *Supplement 1* (April), 2025

Volume 13, *Issue 2* (March-April), 2025

Volume 13, *Issue 1* (January-February), 2025

Explore our developer-friendly HTML to PDF API Printed using PDFCrowd HTML to PDF

2024

Vol. 12

Volume 12, *Supplement 1* (December), 2024

Volume 12, *Issue 6* (November-December), 2024

Volume 12, *Issue 5* (September-October), 2024

Volume 12, *Issue 4* (July-August), 2024

Volume 12, *Issue 3* (May-June), 2024

Volume 12, *Issue 2* (March-April), 2024

Volume 12, *Issue 1* (January-February), 2024

2023

Vol. 11

Volume 11, *Issue 6* (November-December), 2023

Volume 11, *Issue 5* (September-October), 2023

Volume 11, *Issue 4* (July-August), 2023

Volume 11, *Issue 3* (May-June), 2023

Volume 11, *Issue 2* (March-April), 2023

Volume 11, *Issue 1* (January-February), 2023

2022

Vol. 10

Explore our developer-friendly HTML to PDF API Printed using PDFCrowd HTML to PDF

Volume 10, *Supplement 1* (December), 2022 (Abstract Book of ECFA 2022)

Volume 10, *Issue 6* (November-December), 2022

Volume 10, *Issue 5* (September-October), 2022

2021

Vol. 9

Volume 10, *Issue 4* (July-August), 2022

Volume 9, *Issue 6* (November-December), 2021

Volume 10, *Issue 3* (May-June), 2022

Volume 9, *Supplement 1* (October), 2021 (Abstract Book of MICPS 2021)

Volume 10, *Issue 2* (March-April), 2022

Volume 9, Issue 5 (September-October), 2021

Volume 10, *Issue 1* (January-February), 2022

Volume 9, *Issue 4* (July-August), 2021

Volume 9, *Issue 3* (May-June), 2021

Volume 9, *Issue 2* (March-April), 2021

Volume 9, *Issue 1* (January-February), 2021

2020

Vol. 8

Volume 8, *Issue 6* (November-December)

Volume 8, *Issue 5* (September-October)

Volume 8, *Issue 4* (July-August)

Volume 8, *Issue 3* (May-June)

Volume 8, *Issue 2* (March-April)

Volume 8, *Issue 1* (January-February)

2019

Vol. 7

Volume 7, *Supplement 2* (November)(Abstract book of LATINFARMA 2019)

Volume 7, *Issue 6* (November-December)

Explore our developer-friendly HTML to PDF API Printed using PDFCrowd HTML to PDF

Volume 7, *Supplement 1* (October)(Abstract book of ZTIPC 2019)

Volume 7, *Issue 5* (September-October)

Volume 7, *Issue 4* (July-August)

Volume 7, *Issue 3* (May-June)

Volume 7, *Issue 2* (March-April)

Volume 7, *Issue 1* (January-February)

2018

Vol. 6

Volume 6, *Issue 6* (November-December)

Volume 6, *Issue 5* (September-October)

Volume 6, *Issue 4* (July-August)

Volume 6, *Issue 3* (May-June)

Volume 6, *Issue 2* (March-April)

Volume 6, *Issue 1* (January-February)

2017

Vol. 5

Volume 5, *Issue 6* (November-December)

Volume 5, *Issue 5* (September-October)

Volume 5, *Issue 4* (July-August)

Volume 5, *Issue 3* (May-June)

Volume 5, *Issue 2* (March-April)

Volume 5, *Issue 1* (January-February)

2016

Explore our developer-friendly HTML to PDF API Printed using PDFCrowd HTML to PDF

Vol. 4

Volume 4, *Issue 6* (November-December)

Volume 4, *Issue 5* (September-October)

Volume 4, *Issue 4* (July-August)

Volume 4, *Issue 3* (May-June)

Volume 4, *Issue 2* (March-April)

Volume 4, *Issue 1* (January-February)

2015

Vol. 3

Volume 3, *Issue 6* (November-December)

Volume 3, *Issue 5* (September-October)

Volume 3, *Supplement 1*, (September)(Abstract book of FAPRONATURA 2015)

Volume 3, *Issue 4* (July-August)

Volume 3, *Issue 3* (May-June)

Volume 3, Issue 2 (March-April)

Volume 3, *Issue 1*, (January-February), 2015

2014

Vol. 2

Volume 2, *Issue 6* (November-December)

Volume 2, *Issue 5* (September-October)

Volume 2, *Issue 4* (July-August)

Volume 2, *Issue 3* (May-June)

Volume 2, *Supplement 1* (May)(Abstract book of LATINFARMA 2013)

Explore our developer-friendly HTML to PDF API Printed using PDFCrowd HTML to PDF

Volume 2, *Issue 2* (March-April)

Volume 2, *Issue 1* (January-February)

2013

Vol. 1

Volume 1, *Issue 2* (November-December)

Volume 1, *Issue 1* (September-October)



© 2013-2020 by the authors; licensee JPPRes, Antofagasta, Chile. This journal is an open-access journal distributed under the terms and conditions of the Creative Commons Attribution license-Non Commercial 4.0 international. The content on this site is intended for health professionals. If you are not a health professional, please talk to your doctor about any doubts or concerns regarding your health

Site Update: October 25th, 2026

Made with ♥ by **AVAGAX Studio**

Explore our developer-friendly HTML to PDF API Printed using PDFCrowd **HTML to PDF**

JPPRes | Journal of Pharmacy & Pharmacognosy Research

Volume 14, Issue 4

J Pharm Pharmacogn Res 14(4), (Jul-Aug) 2026



IFC **(Journal of Pharmacy & Pharmacognosy Research).**

1.- Original Article

Retnaningsih Retnaningsih, Widhy A. Wardhani, Dodik T. Pramukarso (2026) **Association of body mass index with complications and outcomes among intensive care unit stroke patients. |** [Asociación del índice de masa corporal con desenlaces en pacientes con ictus en cuidados intensivos]. J Pharm Pharmacogn Res 14(4): 2539 https://doi.org/10.56499/jppres_14.4.2858 [327 Kb] [ABSTRACT]

2.- Original Article

Warsito Warsito, Elok Zubaidah, Tri Ardyati, Risna Silvianti, Rista N. Rohmah, Aqidatul Izzo (2026) **Eugenyl salicylate nanoemulsion in roselle kombucha: Culturable counts and SCOBY-associated 16S/ITS microbial profiles**. | [Nanoemulsión de salicilato de eugenilo en kombucha de roselle: recuentos cultivables y perfiles 16S/ITS asociados a SCOBY]. J Pharm Pharmacogn Res 14(4): 2703. https://doi.org/10.56499/jppres_14.4.2703 [632 Kb] [ABSTRACT]

3.- Original Article

Sri Ningsih, Nisrina Firdausi, Erni Hernawati Purwaningsih, Sri Widia A. Jusman, Wahono Sumaryono, Lamhot Parulian Manalu, Sjaikhurrizal El Muttaqien, Tarwadi Tarwadi Muhammad Delwar Hussain, Mohsin Kazi (2026) **Hepatoprotective activity of *Uncaria gambir* extract in CCl_4-induced liver fibrosis associated with suppression of TIMP-1 and type I collagen**. | [Actividad hepatoprotectora del extracto de *Uncaria gambir* en ur

Khanh Cong Van, Thuan Thi Duong, Kien Ba Tran (2026) **An assessment of digita transformation maturity among Vietnamese pharmaceutical enterprises: A cross-sectional study**. | [Evaluación de la madurez de la transformación digital en empresas farmacéuticas vietnamitas: un estudio transversal]. J Pharm Pharmacogn Res 14(4) 2568. https://doi.org/10.56499/jppres_14.4.2568 [753 Kb] [ABSTRACT]

5.- Original Article

Suryono Suryono, Muhammad I. Amien, Achmad I. Tohari, Antonius D. Saputra Muhammad R. Fahrudin Hidayat, Muhammad N. Hibatullah, Hazbina F. Ramadhan Muhammad F. Hibatulloh (2026) **Integrated network pharmacology and molecular simulation analysis of colchicine in coronary in-stent restenosis**. | [Análisis integrado de farmacología de redes y simulación molecular de la colchicina en la reestenosis coronaria intrastent]. J Pharm Pharmacogn Res 14(4): 2545 https://doi.org/10.56499/jppres_14.4.2545 [1.50 Mb] [ABSTRACT]

6.- Original Article

Kristiine Roostar, Oleh Koshovyi, Andres Meos, Ivo Laidmäe, Ain Raal, Urve Paaver, Jyrk Heinämäki (2026) **Semi-solid extrusion 3D printing of quercetin-loaded polyethylene oxide–poloxamer gel formulations: A proof-of-concept study**. | [Impresión 3D por extrusión semisólida de formulaciones en gel de óxido de polietileno–poloxámero cargadas con quercetina: estudio de prueba de concepto]. J Pharm Pharmacogn Res 14(4): 2836. https://doi.org/10.56499/jppres_14.4.2836 [1.65 Mb] [ABSTRACT]

7.- Original Article

Ago Harlim, Hulman Panjaitan, Hubert Andrew, Chastine Harlim (2026) **Self-reported implant-site inflammatory reactions after COVID-19 vaccination among Indonesian cosmetic implant recipients: Cross-sectional survey**. | [Reacciones inflamatorias autoinformadas tras vacunación COVID-19 en receptores indonesios de implantes cosméticos: estudio transversal]. J Pharm Pharmacogn Res 14(4): 2722 https://doi.org/10.56499/jppres_14.4.2722 [750 Kb] [ABSTRACT]

8.- Review

Islan Nor, Afrillia N. Garmana, Mohamad Rafi, Youngmin Kang, Muhamad Insanu (2026) ***Durio* species and metabolic syndrome: A systematic review of bioactivity and phytochemistry.** | [Especies de *Durio* y síndrome metabólico: una revisión sistemática

biochemical, immunological, and microbiological alterations associated with cigarette, IQOS, and e-cigarette use. | [Alteraciones salivales asociadas al uso de cigarrillos, IQOS y cigarrillos electrónicos]. J Pharm Pharmacogn Res 14(4): 2702 https://doi.org/10.56499/jppres_14.4.2702 [1.11 Mb] [ABSTRACT]

10.- Original Article

Arif Al Iman, Afrillia Nuryanti Garmana, Defri Rizaldy, Annisa Septianti Sekar Kinasih Sukrasno (2026) **Dermal anti-aging potential of *Coffea canephora* bean aqueous extract: An integrated study *in silico* and *in vitro*.** | [Potencial antienvejecimiento dérmico del extracto acuoso de granos de *Coffea canephora*: un estudio integrado *in vitro* e *in silico*]. J Pharm Pharmacogn Res 14(4): 2840 https://doi.org/10.56499/jppres_14.4.2840 [1.07 Mb] [ABSTRACT]

11.- Original Article

Jauharotus Shobahah, Dwi Winarni, M. Ainun Najib Aly, Naswandi Nur, Win Darmanto, Dwi Hudiyanti, Lionel In Lian Aun, Sri Puji Astuti Wahyuningsih (2026) **Solvent-free β-glucan-coated VD3 nanoliposomes: Physicochemical characterization and preliminary *in vitro* evaluation.** | [Nanoliposomas de vitamina D3 recubiertos con β-glucano y preparados sin disolventes: caracterización fisicoquímica y evaluación preliminar *in vitro*]. J Pharm Pharmacogn Res 14(4): 2654. https://doi.org/10.56499/jppres_14.4.2654 [1.00 Mb] [ABSTRACT]

12.- Original Article

Abu Bakar, Shih-Chieh Lee, Valendriyani Ningrum (2026) **Molecular docking-based screening of bioactive compounds from *Cinnamomum burmanni* against mTORC1 in oral mucositis.** | [Cribado de compuestos bioactivos de *Cinnamomum burmanni* frente a mTORC1 en la mucositis oral mediante acoplamiento molecular]. J Pharm Pharmacogn Res 14(4): 2879. https://doi.org/10.56499/jppres_14.4.2879 [1.42 Mb] [ABSTRACT]

© 2026 Journal of Pharmacy & Pharmacognosy Research (JPPRes)

JPPRes | Journal of Pharmacy & Pharmacognosy Research

Twitter LinkedIn Facebook

© 2013-2020 by the authors; licensee JPPRes, Antofagasta, Chile. This journal is an open-access journal distributed under the terms and conditions of the Creative Commons Attribution license-Non Commercial 4.0 international. The content on this site is intended for health professionals. If you are not a health professional, please talk to your doctor about any doubts or concerns regarding your health

Site Update: October 25th, 2026

Made with ♥ by **AVAGAX Studio**

Editorial Board



Editor-in-Chief:

Gabino Garrido [Scholar Google] [Scopus] [ResearchGate] [ORCID]
Departamento de Ciencias Farmacéuticas
Universidad Catolica del Norte
Antofagasta
Chile
E-mail: editor@jppres.com

Executive Editor:

Marisela Valdés González
Departamento de Ciencias Farmacéuticas
Universidad Catolica del Norte
Antofagasta
Chile

E-mail: jppres12@gmail.com

Editorial and Design Manager:

Xavier Garrido Valdés

AVAGAX - Diseño, Publicidad y Servicios Informáticos
Antofagasta
Chile

Editorial Board Members:

Antonio Vassallo. Dipartimento di Scienze. Università degli Studi della Basilicata, Potenza, Italia. [ResearchGate] [ORCID][Scopus]

Bárbara Beatriz Garrido Suárez. Laboratorio de Farmacología y Toxicología, Centro de Investigación y Desarrollo de Medicamentos, La Habana, Cuba. [ResearchGate]

Carla Delporte. Facultad de Ciencias Químicas y Farmacéuticas, Universidad de Chile, Santiago, Chile. [ResearchGate][ORCID]

Damaris Silveira. Faculdade de Ciências da Saúde, Universidade de Brasília, Brazil. [Lattes][ORCID]

Douglas Siqueira de Almeida Chaves. Dep. de Ciências Farmacêuticas (DCFar), Instituto de Ciências Biológicas e da Saúde, Universidade Federal Rural do Rio de Janeiro, Rodovia, RJ. Brazil. [Lattes][ORCID][ResearchGate]

Edgar Pastene. Universidad de Concepción, Concepción, Chile. [ResearchGate][ORCID]

Etile Spegazzini. Universidad de Belgrano, Buenos Aires, Argentina. [ResearchGate]

Farid Chemat. Université Avignon et des Pays de Vaucluse, Avignon, France [ResearchGate]

Fidel O. Castro. Departamento de Ciencias Pecuarias, Universidad de Concepción, Chillán, Chile. [ResearchGate][ORCID]

Guilherme Nobre L. do Nascimento. Universidade Federal de Tocantins. Brazil. [ORCID][Lattes]

Jacqueline Sepúlveda. Universidad de Concepción, Concepción, Chile

Jelena Nadinic. Universidad de Buenos Aires, Argentina. [ResearchGate]

José H. Isaza-Martínez. Universidad del Valle, Cali, Colombia. [ORCID][ResearchGate]

Juan C. Sepúlveda-Arias. Universidad Tecnológica de Pereira, Pereira, Colombia. [ORCID][ResearchGate]

Madan Mohan Gupta. School of Pharmacy, Faculty of Medical Sciences. The University of the West Indies, Trinidad & Tobago, West Indies. [Google Scholar]

Mahomoodally M. Fawzi. Department of Health Sciences, Faculty of Science, University of Mauritius. Mauritius. [ORCID][ResearchGate]

María Inés Isla. Facultad de Ciencias Naturales e Instituto Miguel Lillo. Universidad Nacional de Tucumán, Tucumán, Argentina. [ORCID] [ResearchGate]

Marisol Fernández Alfonso. Facultad de Farmacia, Universidad Complutense de Madrid, España.[ORCID][ResearchGate]

Mayank Gangwar. Department of Pharmacology, Institute of Medical Sciences, Banaras Hindu University, Varanasi (UP) India. [ORCID][Google Scholar]

Silvia Debenedetti. Pharmacy Carreer. Universidad de Belgrano, Buenos Aires, Argentina. [ORCID][ResearchGate]

Vikash Kumar Ruhil. PDM College of Pharmacy, Bahadurgarh, Haryana, India. [Google Scholar]

Yasser Shahzad. Department of Pharmacy. COMSATS University Islamabad, Pakistan. [ORCID][Scopus][Google Scholar]

Reviewers

The reviewers will be recruited among researchers and clinicians with high international reputation in Pharmacy and Pharmacognosy.

Last Update: December 31, 2021

© 2013-2020 by the authors; licensee JPPRes, Antofagasta, Chile. This journal is an open-access journal distributed under the terms and conditions of the Creative Commons Attribution license-Non Commercial 4.0 international. The content on this site is intended for health professionals. If you are not a health professional, please talk to your doctor about any doubts or concerns regarding your health

Site Update: October 25th, 2026

© 2026 Journal of Pharmacy & Pharmacognosy Research, 14 (4), 2545, 2026
ISSN 0719-4250
https://jppres.com

DOI: https://doi.org/10.56499/jppres_14.4.2545

Original Article

Integrated network pharmacology and molecular simulation analysis of colchicine in coronary in-stent restenosis

[Análisis integrado de farmacología de redes y simulación molecular de la colchicina en la reestenosis coronaria intrastent]

Suryono Suryono[1*], Muhammad I. Amien[2], Achmad I. Tohari[2,3], Antonius D. Saputra[2], Muhammad R. Fahrudin Hidayat[2], Muhammad N. Hibatullah[2], Hazbina F. Ramadhan[4], Muhammad F. Hibatulloh[2]

[1]Department of Cardiology and Vascular Medicine, Faculty of Medicine, Universitas Jember - Dr. Soebandi General Hospital- Jember, Indonesia.
[2]Faculty of Medicine, Universitas Jember, Jember, Indonesia.
[3]Department of Epidemiology and Preventive Medicine, Graduate School of Medical and Dental Sciences, Kagoshima University, Kagoshima, Japan.
[4]Kalisat General Hospital, Jember, Indonesia.
*E-mail: suryonofiha@gmail.com

Abstract

Context: In-stent restenosis (ISR) remains a major complication following percutaneous coronary intervention. Increasing evidence suggests that genetic and inflammatory mechanisms contribute to ISR pathogenesis. Colchicine has demonstrated anti-inflammatory effects in cardiovascular diseases; however, its molecular targets in ISR remain unclear.

Aims: To identify potential molecular targets and signaling pathways through which colchicine may modulate ISR using integrated computational approaches.

Methods: ISR-related genes were retrieved from GeneCards, OMIM, and CTD databases. Colchicine targets were predicted using SwissTargetPrediction, BindingDB, SEASearch, and DrugBank. Overlapping genes were analyzed using protein–protein interaction networks and hub gene identification. Functional enrichment analysis was performed using GO and KEGG pathways. Molecular docking and 200 ns molecular dynamics simulations were conducted to evaluate binding stability. Binding free energies were calculated using MM-GBSA.

Results: Sixteen overlapping targets were identified, and ten hub genes were prioritized. Docking analysis demonstrated moderate binding affinity of colchicine toward CYP3A4, TUBB1, and CYP2B6 (−6.9 to −7.4 kcal/mol). Molecular dynamics simulations indicated stable ligand–protein complexes with RMSD values below 2.5 Å. MM-GBSA analysis suggested favorable binding energies, particularly for TUBB1.

Conclusions: Colchicine was predicted to interact with several ISR-associated targets and pathways, providing a computational basis for further experimental validation.

Keywords: drug repurposing; in-stent restenosis; molecular docking simulation; molecular dynamics simulation; network pharmacology.

Resumen

Contexto: La reestenosis intrastent (ISR) sigue siendo una complicación importante tras la intervención coronaria percutánea. Evidencias crecientes sugieren que los mecanismos genéticos e inflamatorios contribuyen a la patogénesis de la ISR. La colchicina ha demostrado efectos antiinflamatorios en enfermedades cardiovasculares; sin embargo, sus dianas moleculares en la ISR aún no están completamente aclaradas.

Objetivos: Identificar posibles dianas moleculares y vías de señalización a través de las cuales la colchicina podría modular la ISR mediante enfoques computacionales integrados.

Métodos: Los genes relacionados con la ISR se obtuvieron de las bases de datos GeneCards, OMIM y CTD. Las dianas de la colchicina se predijeron mediante SwissTargetPrediction, BindingDB, SEA Search y DrugBank. Los genes superpuestos se analizaron mediante redes de interacción proteína-proteína e identificación de genes centrales (hub genes). El análisis de enriquecimiento funcional se realizó mediante las bases de datos GO y KEGG. Se llevaron a cabo estudios de acoplamiento molecular y simulaciones de dinámica molecular de 200 ns para evaluar la estabilidad de la unión. Las energías libres de unión se calcularon mediante MM-GBSA.

Resultados: Se identificaron dieciséis dianas superpuestas y se priorizaron diez genes centrales. El análisis de acoplamiento mostró una afinidad de unión moderada de la colchicina para CYP3A4, TUBB1 y CYP2B6 (−6,9 a −7,4 kcal/mol). Las simulaciones de dinámica molecular indicaron complejos ligando-proteína estables, con valores de RMSD inferiores a 2,5 Å. El análisis MM-GBSA indicó energías de unión favorables, en particular para TUBB1.

Conclusiones: La colchicina podría interactuar con múltiples dianas relacionadas con la ISR y proporcionar una base computacional para estudios posteriores de validación experimental.

Palabras Clave: acoplamiento molecular; dinámica molecular; farmacología de redes; reestenosis intrastent; reposicionamiento de fármacos.

ARTICLE INFO
Received: August 7, 2025.
Accepted: July 28, 2026.
Available Online: August 9, 2026.

AUTHOR INFO
ORCID: 0000-0001-9022-9674 (SS) 0000-0002-5956-6805 (MRFH)
0000-0002-5672-6957 (MIA) 0000-0002-3562-3887 (HFR)
0000-0003-4465-2011 (AIT) 0009-0008-5526-1992 (MNH)
0000-0001-7356-6732 (ADS) 0009-0008-7711-8644 (MFH)

Abbreviations: ABCB1: ATP binding cassette subfamily b member 1; **ADMET**: Absorption, distribution, metabolism, excretion, and toxicity; **ALB**: Albumin; **CHARMM**: Chemistry at HARvard Macromolecular Mechanics; **CTD**: Comparative toxicogenomics database; **CYP**: Cytochrome P450; **DES**: Drug-eluting stent; **DMNC**: Density of maximum neighborhood component; **FDR**: False discovery rate; **FU**: Fraction unbound; **GO**: Gene ontology; **HDAC**: Histone deacetylase; **IL**: Interleukin; **ISR**: In-stent restenosis; **KEGG**: Kyoto Encyclopedia of Genes and Genomes; **MCC**: Maximal clique centrality; **MD**: Molecular dynamics; **MITF**: Microphthalmia-associated transcription factor; **MM-GBSA**: Molecular mechanics generalized born surface area; **MNC**: Maximum neighborhood component; **NR0B1**: Nuclear receptor subfamily 0 group b member 1; **NR1I2**: Nuclear receptor subfamily 1 group i member 2; **OMIM**: Online Mendelian inheritance in man; **PDB**: Protein data bank; **P-gp**: P-glycoprotein; **PPI**: Protein-protein interaction; **Rg**: Radius of gyration; **RMSD**: Root mean square deviation; **RMSF**: Root mean square fluctuation; **SASA**: Solvent accessible surface area; **STRING**: Search tool for the retrieval of interacting genes/proteins; **TC**: Tanimoto coefficient; **TNF-α**: Tumor necrosis factor alpha; **TUBB1**: Tubulin beta-1 chain; **VSMC**: Vascular smooth muscle cell.

INTRODUCTION

In-stent restenosis (ISR) is commonly defined as ≥50% luminal diameter narrowing within a previously implanted stent or within the adjacent 5 mm stent-edge segments proximally or distally ("stent edges") of a previously implanted stent (Alfonso et al., 2022). Bare metal stents (BMSs) led to more predictable outcomes and reduced restenosis. Nevertheless, 1-year incidences of ISR remained around 20–30%, mainly due to exaggerated neointimal proliferation (Zhang & Chen, 2020). It refers to luminal narrowing that involves the proliferation and migration of vascular smooth muscle cells (VSMCs). This process is initiated by endothelial injury during percutaneous coronary intervention or stent implantation, which induces infiltration of inflammatory cells, including monocytes, macrophages, neutrophils, and lymphocytes, leading to the release of cytokines such as interleukin (IL)-1, IL-6, and tumor necrosis factor alpha (TNF-α). Subsequently, VSMCs are activated, and these cytokines promote neointimal hyperplasia (Curcio et al., 2011). Drug-eluting stents (DESs), which are designed to release an antiproliferative medication including sirolimus (rapamycin), zotarolimus, everolimus, and paclitaxel, have substantially reduced ISR at 1-year incidences ranging from 2 to 4% to approximately 10%, depending on the individual risk profile and coronary artery disease complexity (Cassese et al., 2015). However, although the application of DES has reduced the incidence of ISR, several studies have shown the delayed mechanisms of neointimal proliferation, neo-atherosclerosis, and local hypersensitivity reactions leading to persistently significant incidences of ISR (Park et al., 2006), and has made it challenging for cardiac interventionists to determine the underlying causes and appropriate therapy. Besides the technical factor of stent placement, recently, restenosis has also been reported to be influenced by genetic factors, particularly in high-risk groups. The genetic characteristics of restenosis have been studied primarily in European populations. The ethnic variability of genetic markers is well known, as shown by the results of the Genetic Determinants of Restenosis (GENDER) study reported by Verschuren et al. (2012). Therefore, potential therapeutic genes associated with ISR may be identified, although such identification remains challenging.

Colchicine has recently emerged as a promising preventive and therapeutic agent for cardiovascular diseases. Colchicine has been reported to reduce proinflammatory cytokine release, inhibit vessel narrowing, and prevent tissue fibrosis in some cardiovascular diseases (Suryono et al., 2023). This drug may contribute to the inhibition of neointimal proliferation by suppressing inflammatory processes and inhibiting VSMC activation. However, the effects of colchicine and its specific role in the preventive treatment of ISR have not been fully elucidated. Therefore, an *in silico* study involving network pharmacology, molecular docking, and molecular dynamics (MD) simulations was employed to identify potential genes related to ISR pathogenesis that may serve as targets, especially for colchicine, and to elucidate the mechanisms and potential relevance of colchicine to ISR-associated mechanisms.

MATERIAL AND METHODS

Network pharmacology

ISR-related gene screening

ISR-related target genes were identified from GeneCards with a probability relevance score cut-off of ≥10, Online Mendelian Inheritance in Man (OMIM), and Comparative Toxicogenomics Database (CTD) with probability inference score cut-offs of ≥3.0. All databases were accessed on 15 June 2026. Searches were conducted on all three platforms using the keyword 'coronary restenosis' and restricting results to *Homo sapiens*. The retrieved results were consolidated, duplicates were excluded, and gene names were standardized through the UniProt database.

Identification of colchicine's gene targets

Colchicine's standard SDF format was downloaded from PubChem and utilized as input in the SwissTargetPrediction platform with a probability cut-off value of ≥0.1 (Cao et al., 2021), BindingDB with a max

similarity value of ≥0.4, SEAsearch with a max Tanimoto Coefficient (TC) of ≥0.7, and Drugbank.

Protein-protein interaction network (PPIN) and hub gene analysis

Overlapping gene targets of colchicine and ISR were identified using Venny 2.1.0. The intersecting genes were then uploaded to the Search Tool for the Retrieval of Interacting Genes/Proteins (STRING) database to construct a protein–protein interaction (PPI) network, with the organism set as *Homo sapiens* and a confidence score ≥0.4. The resulting interaction data were exported and visualized in Cytoscape 3.10.3. Network topology was analyzed with the Cytoscape Analyzer plugin, and key hub genes were identified using the CytoHubba plugin based on the Maximal Clique Centrality (MCC), Maximum Neighborhood Component (MNC), Density of Maximum Neighborhood Component (DMNC), Degree, and clustering coefficient algorithm, to determine potential core targets of colchicine in the prevention of ISR.

GO and KEGG pathway functional enrichment analysis

To assess the functional roles of the core genes associated with colchicine in the prevention of ISR, gene ontology (GO) analysis (biological processes, molecular functions, and cellular components) and Kyoto Encyclopedia of Genes and Genomes (KEGG) pathway enrichment were conducted using the DAVID database and ShinyGO version 0.82. Enrichment results were filtered using a false discovery rate (FDR) threshold of <0.05. The FDR, representing the adjusted p-value, was applied to determine the significance of each enriched term.

Molecular docking

Selection of ligands

The three-dimensional structure of colchicine (PubChem CID: 6167), selected as the primary ligand for this study, was downloaded from the PubChem database. Evaluation based on Lipinski's Rule of Five indicated that colchicine possesses drug-like properties, including a molecular weight below 500 Da, fewer than five hydrogen bond donors, fewer than ten hydrogen bond acceptors, a Log P value under 5, and a polar surface area of less than 140 Å². These parameters, retrieved from PubChem and determined using the Tanimoto coefficient and dictionary-based binary fingerprint method (Kim et al., 2023; Suryono et al., 2025), suggest favorable oral bioavailability. The SDF file was subsequently converted into Protein Data Bank (PDB) format for downstream analysis.

Selection of target proteins

Three potential target proteins, cytochrome P450 (CYP) 3A4, tubulin beta-1 chain (TUBB1), and CYP2B6, were selected based on prior network pharmacology analysis, as they represent the top core genes associated with colchicine and are implicated in the pathogenesis of in-stent restenosis (ISR). The crystal structures of these proteins, namely CYP3A4 (PDB ID: 9MS1), TUBB1 (UniProt ID: Q9H4B7), and CYP2B6 (PDB ID: 4I91), each complexed with a native inhibitor, were retrieved from the RCSB Protein Data Bank and UniProt database, and saved in PDB file format. Further structural examination—including identification of functional domains, as well as the number and identity of amino acid residues within the active sites—was performed using BIOVIA Discovery Studio Visualizer 2021.

Ligand and targets preparation

Preparation of colchicine as the primary ligand was carried out using AutoDock MGL Tools by optimizing ionization states, torsion angles, degrees of freedom, and stereochemical configurations. Gasteiger charges and polar hydrogens were added, and rotatable bonds were defined before the ligand was saved in Protein Data Bank, Partial Charge, and Atom Type Format (PDBQT) format. The target proteins, CYP3A4, TUBB1, and CYP2B6, were processed by removing water molecules and co-crystallized ligands, followed by identification of active site amino acid residues using BIOVIA Discovery Studio Visualizer. Subsequently, Kollman charges and polar hydrogens were added using AutoDock Tools to complete the preparation of receptor structures for docking analysis.

Molecular docking analysis

Molecular docking analysis was conducted using PyRx, which incorporates the AutoDock Vina engine (Amien et al., 2026; Trott & Olson, 2010) to evaluate the binding affinity (expressed in kcal/mol) and characterize the types of interactions formed between the ligand and the target proteins. Prior to docking colchicine to its selected targets, a validation step was performed by redocking the native ligands into the binding sites of CYP3A4, TUBB1, and CYP2B6 to confirm the reliability of the docking protocol. The molecular interactions between colchicine and the three-dimensional structures of these targets were subsequently visualized using PyMol and BIOVIA Discovery Studio Visualizer.

Molecular docking simulations between colchicine and the three potential targets, namely CYP3A4, TUBB1, and CYP2B6, were conducted using the PyRx platform. The exhaustiveness parameter value of the docking process was 8. The grid box parameters applied for the colchicine–CYP3A4 complex were center_x = 19.9680083547, center_y = 22.1337876708,

center_z = 10.7291756388, with size_x = 35.1255421128, size_y = 36.3449223344, and size_z = 38.2163844779. For the colchicine–TUBB1 complex, the parameters were center_x = −3.51801937765, center_y = −1.20356562323, center_z = 0.645811217072, with size_x = 39.0880344265, size_y = 38.7325116849, and size_z = 38.2808529067. Meanwhile, the colchicine–CYP2B6 complex employed center_x = 19.9680083547, center_y = 22.1337876708, center_z = 10.7291756388, with size_x = 35.1255421128, size_y = 36.3449223344, and size_z = 38.2163844779.

Molecular dynamics simulations

The optimal docking conformations demonstrated stable interactions between colchicine and each target receptor, as visualized using BIOVIA Discovery Studio, where hydrogen bonds were added to the ligand–receptor complexes and subsequently saved in PDB format. Topology files and associated parameters for each complex were generated using the Chemistry at HARvard Macromolecular Mechanics (CHARMM-GUI) platform () (Jo et al., 2008). Molecular dynamics (MD) simulations were then performed using Nanoscale Molecular Dynamics (NAMD) software (Phillips et al., 2020). The simulation workflow included energy minimization, equilibration, and production phases. All complexes were solvated in a cubic box using the Transferable Intermolecular Potential with 3 Points (TIP3P) water model. Energy minimization was performed using the Steepest Descent algorithm under the CHARMM36 force field until convergence was achieved. Subsequently, the systems were equilibrated under constant number of particles, volume, and temperature (NVT ensemble) at 310 K for 1 ns using the modified Berendsen (V-rescale) thermostat, followed by equilibration under constant number of particles, pressure, and temperature (NPT ensemble) at 310 K and 1 atm for 1 ns using the Parrinello–Rahman barostat. Long-range electrostatic interactions were calculated using the Particle Mesh Ewald (PME) method with a real-space cutoff of 1.0 nm, while van der Waals interactions were treated with a cutoff distance of 1.0 nm. All covalent bonds involving hydrogen atoms were constrained using the LINCS algorithm. Molecular dynamics simulations were subsequently carried out for 200 ns with a time step of 2 fs. Trajectory coordinates were recorded every 10 ps for subsequent analyses (Hijazi et al., 2018). Post-simulation analyses included calculation of the root mean square deviation (RMSD), root mean square fluctuation (RMSF), Radius of gyration (Rg), and solvent-accessible surface area (SASA) throughout the 200 ns simulation period, which were visualized using Visual Molecular Dynamics (VMD). In addition, the binding free energies of the ligand–receptor complexes were calculated using the Molecular Mechanics–Generalized Born Surface Area (MM-GBSA) approach implemented in AmberTools (Case et al., 2023). To ensure reliable energy estimation, a total of 500 trajectory frames were extracted at 100 ps intervals from the final 50 ns (150–200 ns) of each 200 ns production trajectory and used for MM-GBSA calculations. The entropic contribution (–TΔS) was not included in the MM-GBSA calculations due to the high computational cost and uncertainty associated with entropy estimation.

$$\Delta Gbind = \Delta EvdW + \Delta Eele + \Delta Gpolar + \Delta Gnonpolar \quad [1]$$

where ΔH represents enthalpy change, E_Van der Waals and E_elec refer to van der Waals and electrostatic interaction energies, respectively, while E_sol(gb) and E_np represent polar and non-polar solvation energies.

ADMET prediction

The pharmacokinetic, ADMET, and toxicity profiles of colchicine (SMILES: CC(=O)N[C@H]1CCC2=CC(=C(C(=C2C3=CC=C(C(=O)C=C13)OC)OC)OC)OC) were evaluated using the ADMETlab 3.0 tools. The assessed parameters comprised bioavailability, human intestinal absorption, plasma protein binding, blood–brain barrier penetration, hepatotoxicity, cardiotoxicity, and carcinogenic potential. Favorable ADMET characteristics were indicated by compliance with the Lipinski rule of five, as previously described, together with high human intestinal absorption, strong plasma protein binding (>90%), efficient brain penetration, and low-to-moderate clearance values (5–20%).

A summary of the workflow of this study can be seen in Fig. 1.

RESULTS

Network pharmacology analysis

Identification of ISR-related genes

The keyword “coronary restenosis” was imported to retrieve ISR-related gene targets from the GeneCards, OMIM, NCBI, and CTD databases. The union set of gene targets, comprising 177 targets from GeneCards, 18 targets from OMIM-NCBI, and 8,243 targets from CTD, was subsequently compiled, followed by the removal of duplicate entries. Thereafter, a total of 8,438 putative genes associated with ISR were identified (Supplementary Table 1 and Fig. 2).

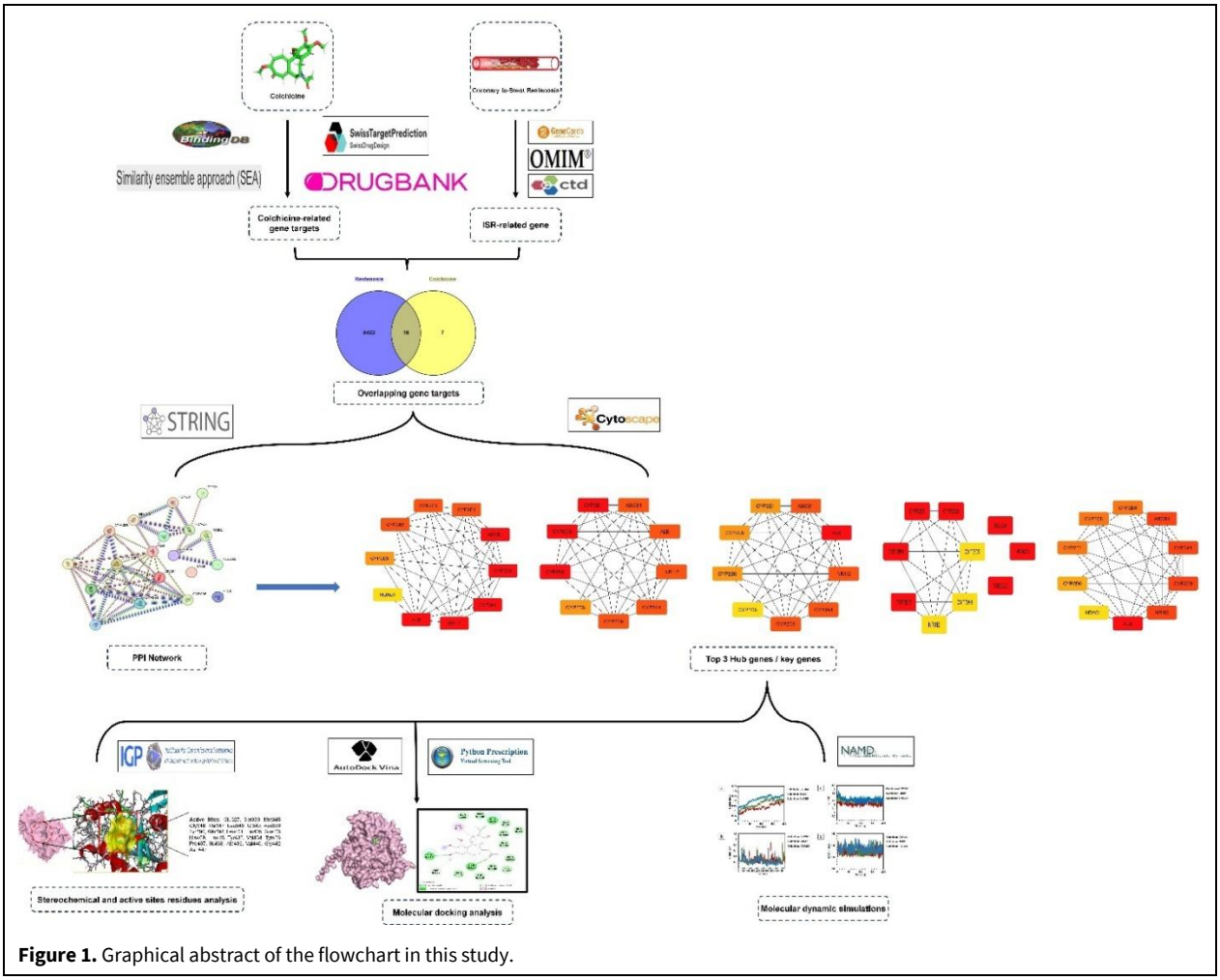


Figure 1. Graphical abstract of the flowchart in this study.

Table 1. Summary of the lowest binding affinity from molecular docking results and the type of interaction of colchicine with the top 3 core targets.

Ligand	Target protein	Grid box (binding pocket) coordinates	Binding affinity (kcal/mol)	Interactions of colchicine and involved residues
Colchicine	CYP3A4	• center_x = 19.9680083547 • center_y = 22.1337876708 • center_z = 10.7291756388 • size_x = 35.1255421128 • size_y = 36.3449223344 • size_z = 38.2163844779	-7.1	**Conventional Hbon**: - **C–H hydrogen bond:** - **Van der Waals**: Asp76, Arg105, Phe108, Thr224, Ala370, Met371, Leu373, Gly481, Leu482
	TUBB1	• center_x = −3.51801937765 • center_y = −1.20356562323 • center_z = 0.645811217072 • size_x = 39.0880344265 • size_y = 38.7325116849 • size_z = 38.2808529067.	-7.4	**Conventional Hbon**: Gln11, Ser138, Tyr222 **C–H hydrogen bond**: Ser138, Asp177 **Van der Waals**: Gly10, Gly13, Gln15, Gly140, Gly141, Thr143, Gly144, Val169, Ser176, Thr178, Asn204
	CYP2B6	• center_x = 19.9680083547 • center_y = 22.1337876708 • center_z = 10.7291756388 • size_x = 35.1255421128 • size_y = 36.3449223344 • size_z = 38.2163844779	-6.9	**Conventional Hbon**: Glu143 **C–H hydrogen bond:** Val129, Ser141 **Van der Waals**: Met132, Phe135, Leu340, Leu437, Gly440, Ile441

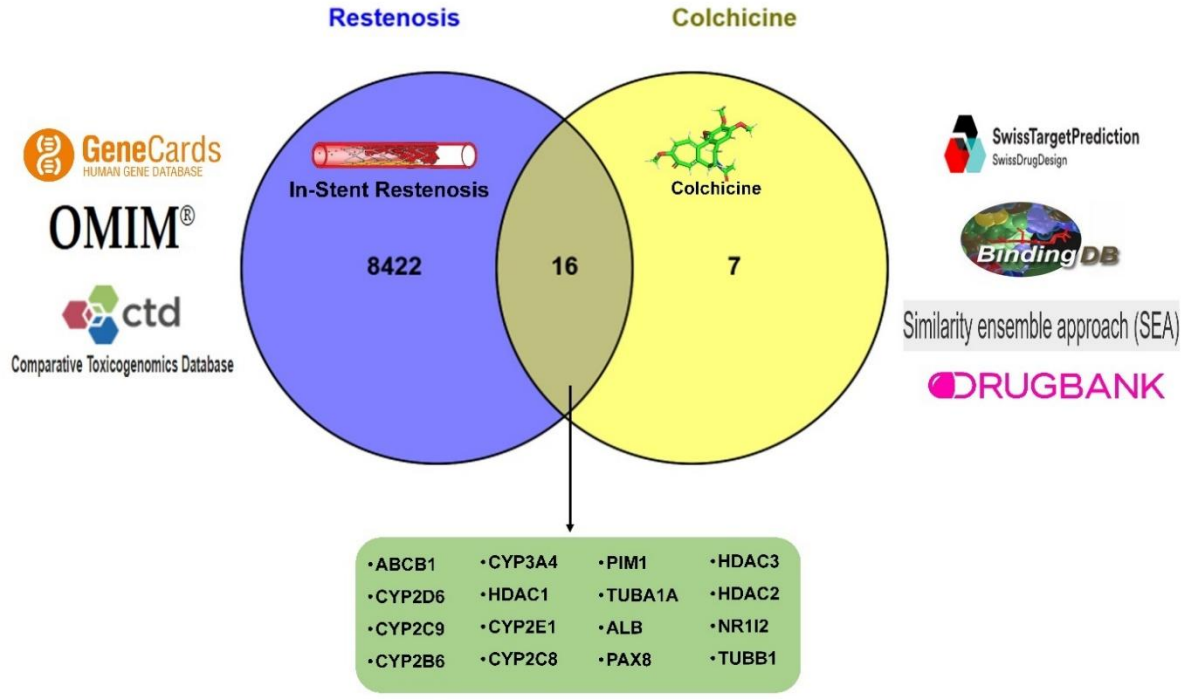


Figure 2. ISR-related genes, colchicine's gene targets, and the common overlapping gene targets between them as potential gene targets for colchicine in the preventive treatment of ISR.

Table 2. The RMSD, RMSF, Rg, and SASA values for simulation trajectories throughout 200ns of production runs.

Receptor-ligand complex	RMSD	RMSF	Rg	SASA
	Mean (nm)	Mean (nm)	Mean (nm)	Mean (nm^2)
Colchicine-CYP3A4	0.132 ± 0.035	0.29	2.23 ± 0.38	130.26 ± 8.05
Colchicine-TUBB1	0.172 ± 0.039	0.27	2.50 ± 0.27	132.2 ± 8.58
Colchicine-CYP2B6	0.21 ± 0.0417	0.23	2.58 ± 0.35	135.14 ± 8.53

Identification of colchicine's gene targets

Based on gene target identification using Swiss TargetPrediction, 5 colchicine gene targets with a probability cut-off≥0.1 are TUBB1, histone deacetylase (HDAC) HDAC6, HDAC1, HDAC3, and HDAC2. From the BindingDB database, there are 8 colchicine gene targets with a max similarity value of ≥0.4, which are HDAC2, HDAC3, Nuclear Receptor Subfamily 0 Group B Member 1 (NR0B1), Nuclear Receptor Subfamily 1 Group I Member 2 (NR1I2), TUBA1A, SLC22A3, TUBB2B, and TPPP. According to the SEASearch database, 12 colchicine gene targets have a maximum TC value ≥ 0.7: TUBA1A, TPPP, TUBB, SLC22A3, PAX8, microphthalmia-associated transcription factor (MITF), CYP2C9, CYP2D6, PIM1, TUBB1, and NR0B1. According to the DrugBank database, there are 7 colchicine gene targets: TUBB, CYP2B6, CYP2C8, CYP2E1, CYP3A4, albumin (ALB), and ABCB1. After that, the union of colchicine's gene targets from these databases was analyzed, and 23 genes obtained, which are HDAC6, HDAC1, HDAC3, HDAC2, NR1I2, TUBB2B, TUBB1, NR0B1, TUBA1A, SLC22A3, TPPP, TUBB, PAX8, MITF, CYP2C9, CYP2D6, PIM1, CYP2B6, CYP2C8, CYP2E1, CYP3A4, ALB, and ABCB1 (Supplementary Table 2).

Finally, the overlapping genes between ISR-related genes obtained before and colchicine's gene targets were identified via Venny 2.1.0, and 16 potential gene targets for colchicine that are involved in the pathogenesis of ISR were obtained which are ABCB1, CYP2D6, CYP2C9, CYP2B6, CYP3A4, HDAC1, CYP2E1, CYP2C8, PIM1, TUBA1A, ALB, PAX8, HDAC3, HDAC2, NR1I2, and TUBB1 (Supplementary Table 3 and Fig. 2).

Table 3. The binding free energy of colchicine with the top 3 core targets.

Ligand-receptor complex	$E_{Van\ der\ Waals}$ (kcal/mol)	E_{ele} (kcal/mol)	$E_{sol(gb)}$ (kcal/mol)	E_{np} (kcal/mol)	$\Delta G_{bind(gb)}$ (kcal/mol)
			(mean ± SD)		
Colchicine-CYP3A4	-36.76 ± 3.61	-14.32 ± 3.66	22.41 ± 2.07	-2.99 ± 0.67	−31.66 ± 5.58
Colchicine-TUBB1	-39.84 ± 4.13	-15.43 ± 2.81	21.87 ± 3.06	-3.34 ± 0.14	−36.74 ± 5.86
Colchicine-CYP2B6	-31.54 ± 3.69	-13.38 ± 4.21	24.46 ± 3.13	-2.68 ± 0.41	−23.14 ± 6.43

*EVan der Waals: van der Waals interaction energy; Eelec: electrostatic interaction energy; Esol (gb): polar solvation energy (GB model); and Enp: non-polar solvation energy; ΔG bind(gb): binding free energy (GB model).

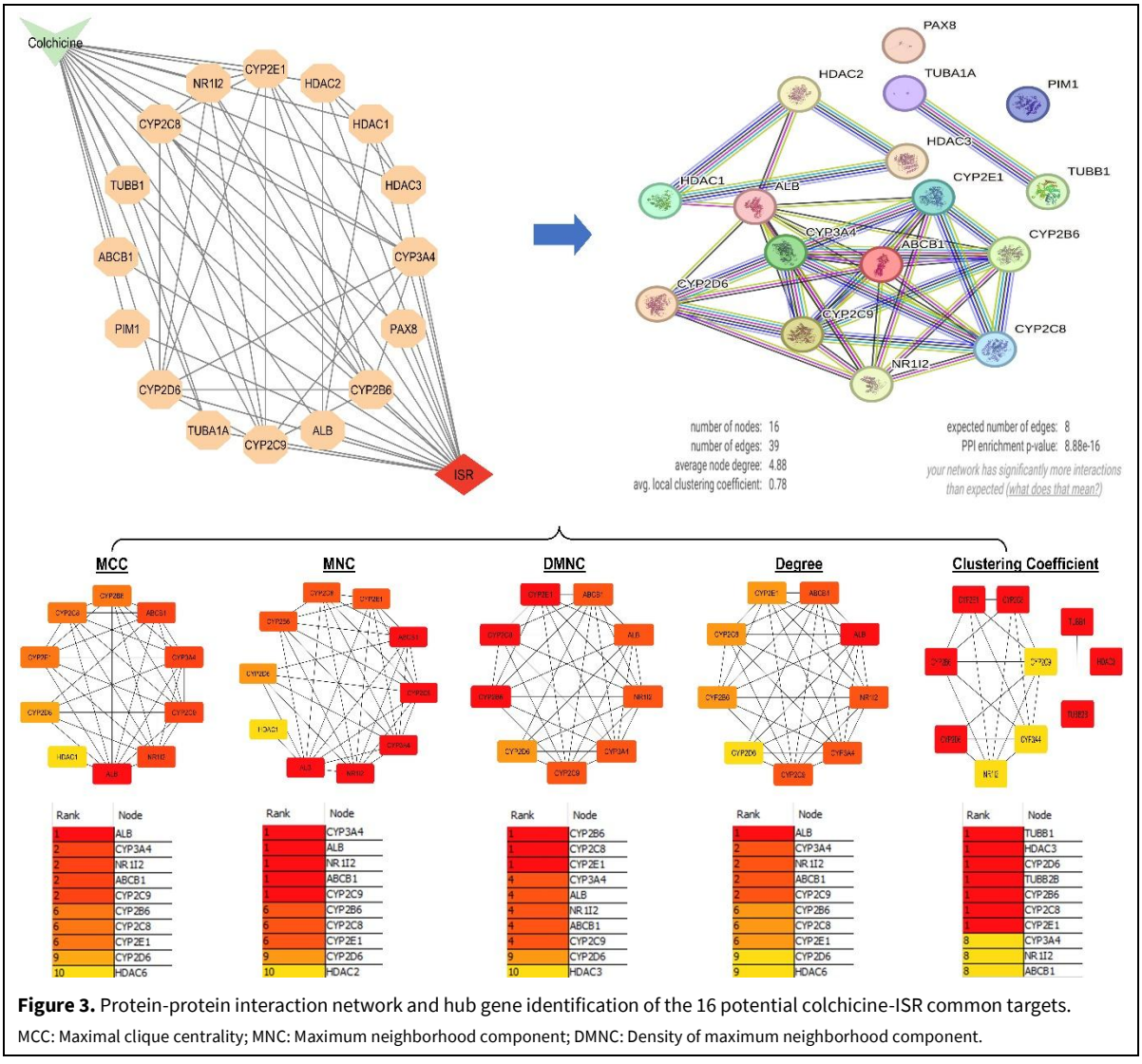


Figure 3. Protein-protein interaction network and hub gene identification of the 16 potential colchicine-ISR common targets.

MCC: Maximal clique centrality; MNC: Maximum neighborhood component; DMNC: Density of maximum neighborhood component.

PPI network construction and hub genes identification

After the ISR-related targets and colchicine's gene targets were intersected, 16 potential colchicine-ISR common targets were obtained (Supplementary Table 3). The STRING tools were used to identify PPIs for 16 potential colchicine targets related to ISR treatment. PPI network showed a total of 16 nodes and 39 edges, with an average local clustering coefficient of 0.78 and a PPI enrichment p-value of 8.88e-16, indicating these 16 proteins have more interactions among themselves than would be expected for a random set of proteins of the same size and degree distribution drawn from the genome. The nodes represented proteins, and the edges represented protein interactions (Fig. 3). Subsequently, the STRING results were imported into Cytoscape and CytoHubba to identify hub genes and core targets of colchicine in the treatment of ISR. Hub genes were prioritized using MCC, DMNC, MNC, Degree, and clustering coefficient algorithms to identify the core target from 16 potential colchicine-ISR common targets using CytoHubba. The results indicated that the most promising common targets identified across

the five CytoHubba algorithms were CYP3A4, TUBB1, and CYP2B6. The ALB protein was excluded from further analysis because it is widely recognized as a non-specific carrier protein involved in drug transport within the systemic circulation (Fig. 3).

Functional enrichment analysis

Based on functional enrichment analysis of the 16 potential colchicine-ISR common targets, GO enrichment revealed the GO entries with the FDR < 0.05 of biological processes (BP), cellular components (CC), and KEGG pathways (Fig. 4). The BP enrichment analysis showed that the overlapping targets were enriched in epoxygenase p40 pathways, arachidonate metabolic process, long chain fatty acid metabolic process, and steroid metabolic process (Fig. 4a). The results suggested that 16 potential colchicine-ISR common targets were concentrated on arachidonate and long chain fatty acid metabolic process (Fig. 4).

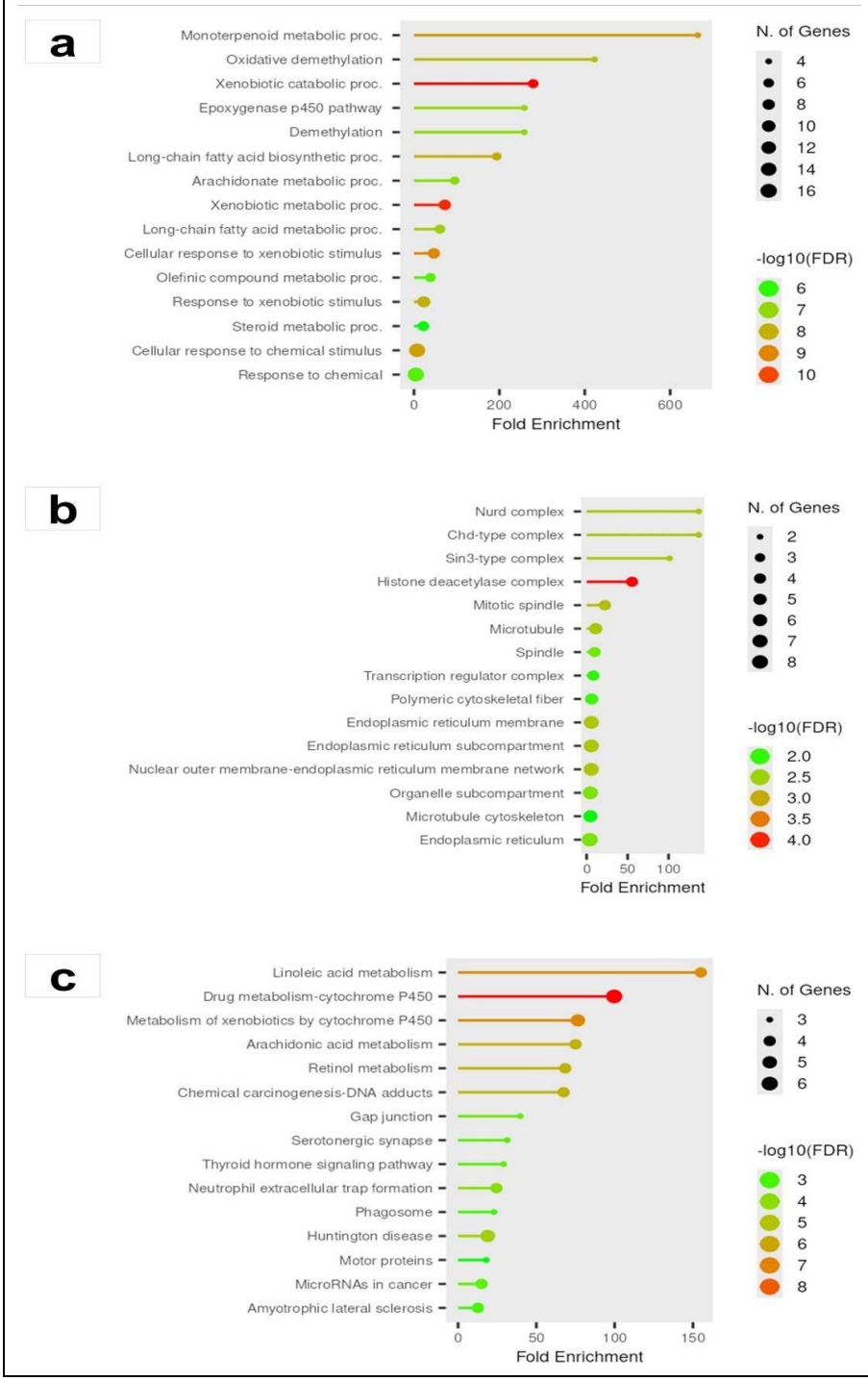


Figure 4. Functional enrichment analysis with an FDR < 0.05 of **(a)** Biological process, **(b)** Cellular component**,** and **(c)** KEGG pathway.

The red node indicates the most significant FDR value, followed by the orange, brown, and green nodes.

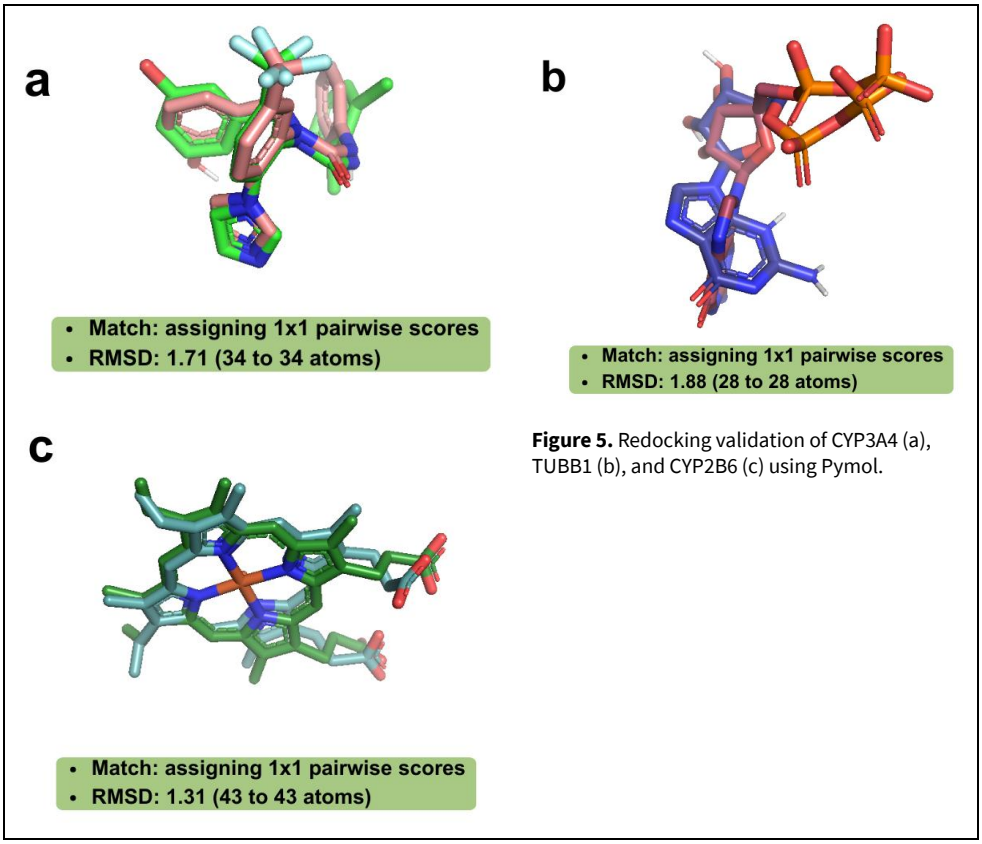


Figure 5. Redocking validation of CYP3A4 (a), TUBB1 (b), and CYP2B6 (c) using Pymol.

Molecular docking

The molecular docking analysis was performed using the top 3 colchicine-ISR core targets, which are CYP3A4, TUBB1, and CYP2B6, to evaluate the binding strength and the interaction of colchicine with those core targets. Native ligands (N'-(2-chlorophenyl)-N-[(3-hydroxyphenyl)methyl]-N-[(2P)-2-(1H-imidazol-1-yl)-5-(trifluoromethyl)phenyl]urea/A1BNX; guanosine-5'-diphosphate/GDP; and protoporphyrin IX containing Fe/HEM) were redocked into the binding pockets of CYP3A4, TUBB1, and CYP2B6 with the same grid box as colchicine. RMSD values between crystallographic and predicted poses were 1.85 Å, 1.94 Å, and 1.32 Å, respectively (Fig. 5; Annex 1), indicating good agreement between the predicted and experimental binding poses. Therefore, the docking protocol was considered valid and suitable for subsequent molecular docking studies. Before the docking process, the target protein's structure must be analyzed and its active sites identified. CYP3A4 (chain A) has some essential amino acid residues as the active-site residues involved in ligand recognition and binding, which are Tyr53, Phe57, Asp76, Arg105, Arg106, Pro10, Phe108, Ile118, Ser119, Ile120, Trp126, Arg130, Phe137, Lys173 Phe220, Val240, Phe241, Phe271, Ile300, Ile301, Phe302, Phe304, Ala305, Glu308, Thr309, Ser312, Val313, Leu364, Ile369, Ala370, Met371, Arg372, Leu373, Glu374, Arg375, Pro434, Phe435, Arg440, Asn441, Cys442, Ile443, Gly444, Phe447, Ala448 (Fig. 6a).

Meanwhile, TUBB1 (chain A) also has some active sites residues which are Arg2, Ile9, Gly10, Gln11, Cys12, Val49, Asp67, Glu69, Gly96, Ala97, Gly98, Asn99, Ser138, Gly140, Gly142, Thr143, Gly144, Val169, Met170, Ser176, Asp177, Thr178, Glu181, Ile193, Ala196, Asp197, Asn204, Ala206, Ile210, Arg213, Leu215, Tyr222, Asn226, Leu231, Leu240, Leu246, Ala248, Ala254, Asn256, Val258, Pro261, His264, Phe270, Pro272, Leu273, Thr274, Gln279, Ala296, Arg297, Thr299, Ala301, Ala302, Cys303, Ala314, Cys315, Lys350, Ala352, Leu361 (Fig. 6b). Lastly, the active binding sites of CYP2B6 (chain A) are Met46, Asp47, Arg49, Gly50, Leu51, Leu52, Lys53, Ser54, Leu56, Arg98, Ile101, Val104, Phe108, Val113, Ile114, Phe115, Trp121, Arg125, Met132, Arg133, Asp166, Phe169, Gln172, Ala176, Ile179, Cys180, Phe184, Phe188, Phe195, Leu199, Phe202, Tyr203, Phe206, Ile209, Leu219, Ile241, Tyr244, Ile245, Leu295, Phe296, Phe297, Ala298, Gly299, Thr302, Thr303, Gln357, Asp361, Leu362, Leu363, Gly366, Val367, His369, Leu392, Ser393, His397, Asp406, Phe426, Ile427, Pro428, Phe429, Ser430, Leu431, Arg434, Cys436, Leu437, Gly438, Glu439, Gly440, Ile441, Glu445, Cys475 (Fig. 6c).

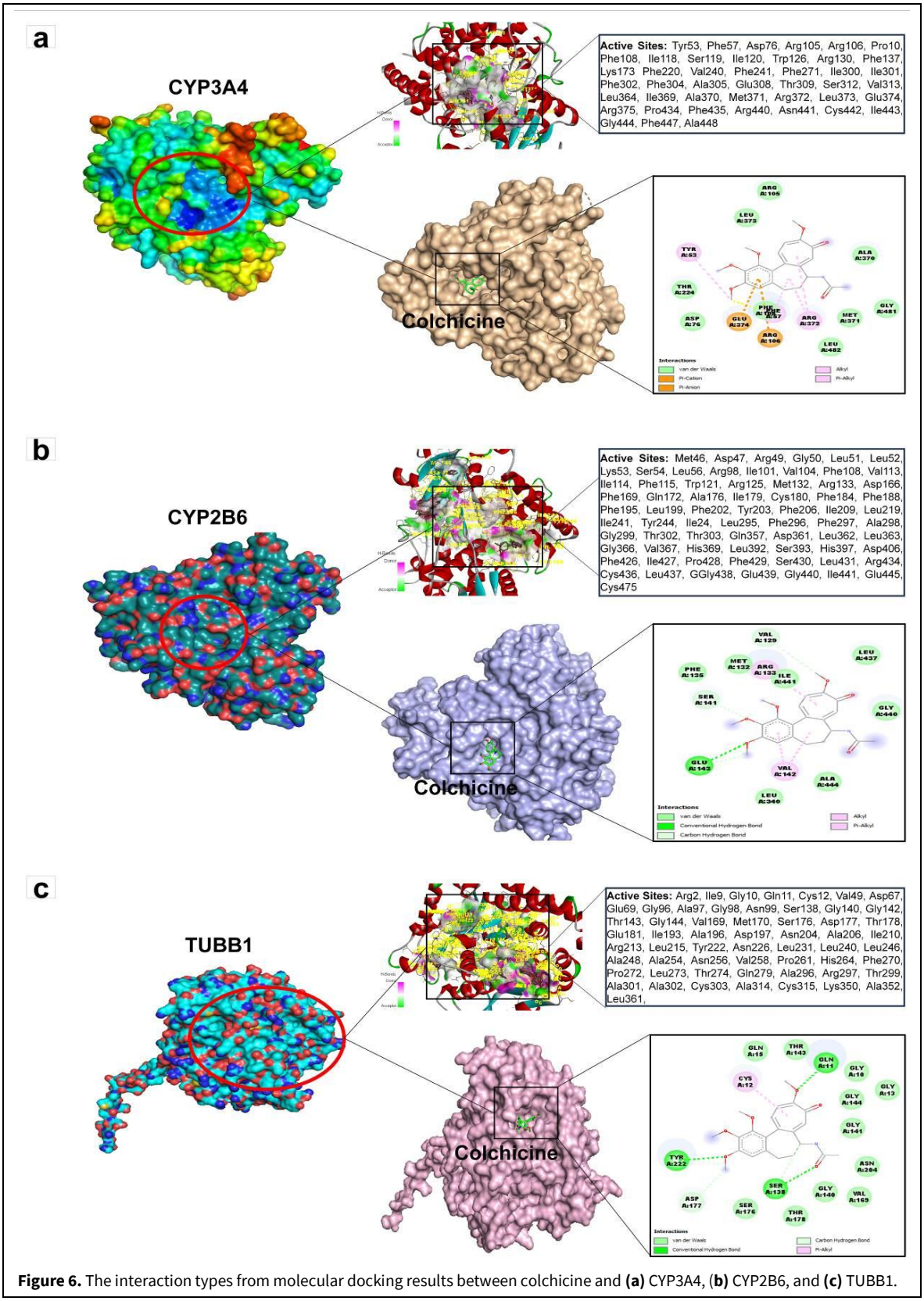


Figure 6. The interaction types from molecular docking results between colchicine and **(a)** CYP3A4, (**b)** CYP2B6, and **(c)** TUBB1.

The molecular docking results showed that colchicine could bind to the active sites of CYP3A4 through Van der Waals interactions with Asp76, Arg105, Phe108, Thr224, Ala370, Met371, Leu373, Gly481, Leu482; with the binding affinity of -7.1 kcal/mol (moderate binding) (Fig. 6a). Colchicine also binds to the active sites of TUBB1 through conventional hydrogen bonds with Gln11, Ser138, Tyr222; carbon hydrogen bondwithSer138, Asp177; and Van der Waals interactions with Gly10, Gly13, Gln15, Gly140, Gly141,

Thr143, Gly144, Val169, Ser176, Thr178, Asn204; with the binding affinity of -7.4 kcal/mol (moderate binding) (Fig. 6b). On the other hand, colchicine also interacts with the active sites of CYP2B6 through conventional hydrogen bonds with Glu143; carbon hydrogen bondwithVal129, Ser141; and Van der Waals interactions with Met132, Phe135, Leu340, Leu437, Gly440, Ile441; with the binding affinity of -6.9 kcal/mol (moderate binding) (Fig. 6c). From the overall docking results, colchicine has the lowest binding affinity with TUBB1, followed by CYP3A4 and CYP2B6 (Table 1).

Molecular dynamics simulations

Molecular dynamics (MD) simulations were performed on the docked complex of colchicine and the top 3 core genes to assess their structural stability under biologically relevant conditions. The system was simulated for 200 ns and subjected to preliminary analyses, including evaluation of RMSD, RMSF, Rg, and SASA. The observed RMSD fluctuations reflected the dynamic stability of the protein-ligand complex, with pronounced deviations indicating structural instability and minor variations suggesting that the system had reached a stable conformation. The results showed that colchicine-CYP3A4, colchicine-TUBB1, and colchicine-CYP2B6 complexes exhibited an initial increasing trend in RMSD during the first 40-50 ns of simulation. Subsequently, fluctuations decreased after 60 ns, indicating convergence toward stable conformations. The mean and corresponding deviations of RMSD values were 0.132 ± 0.035 nm, 0.172 ± 0.039 nm, and 0.21 ± 0.0417 nm for colchicine-CYP3A4, colchicine-TUBB1, and colchicine-CYP2B6, respectively, supporting the overall stability (Fig. 7a). Furthermore, the structural flexibility and compactness of the complexes were evaluated using RMSF and radius of gyration (Rg) analyses. The RMSF values of the colchicine and top 3 core genes complexes ranged from 0.03 to 0.9 nm, with a mean value of 0.29 nm, 0.27 nm, and 0.23 nm for colchicine-CYP3A4, colchicine-TUBB1, and colchicine-CYP2B6 respectively (Fig. 7b). In addition, the colchicine and top 3 core genes complexes displayed a stable Rg profile up after 60 ns simulations, with an average value at the first 60 ns of 2.31 ± 0.37 nm, 2.56 ± 0.29 nm, 2.80 ± 0.43 nm; and after 60 ns yielding an average of 2.23 ± 0.38 nm, 2.50 ± 0.27 nm, and 2.58 ± 0.35 nm for colchicine-CYP3A4, colchicine-TUBB1, and colchicine-CYP2B6 respectively, suggesting increased compactness and sustained structural stability (Fig. 7c). Finally, the SASA analysis showed the average values of 130.26 ± 8.05 nm^2, 132.2 ± 8.58 nm^2, 135.14 ± 8.53 nm^2 for colchicine-CYP3A4, colchicine-TUBB1, and colchicine-CYP2B6 respectively (Fig. 7d).

The binding free energy analysis using the MMGBSA approach: the values are shown in Table 3. The lowest MMGBSA value indicated a stronger binding between the ligand and the target. Based on MMGBSA values, the colchicine-TUBB1 complex has the most favorable predicted binding free energy, with a value of -36.74 ± 5.86 kcal/mol, followed by CYP3A4 and CYP2B6.

ADMET analysis

ADMET analysis demonstrated that colchicine satisfied the Lipinski rule criteria, suggesting its potential suitability as a ligand for target proteins in molecular docking and MD simulation studies. In the absorption profile, colchicine exhibited favorable characteristics, particularly regarding human intestinal absorption, and was predicted not to act as a P-glycoprotein (P-gp) inhibitor.

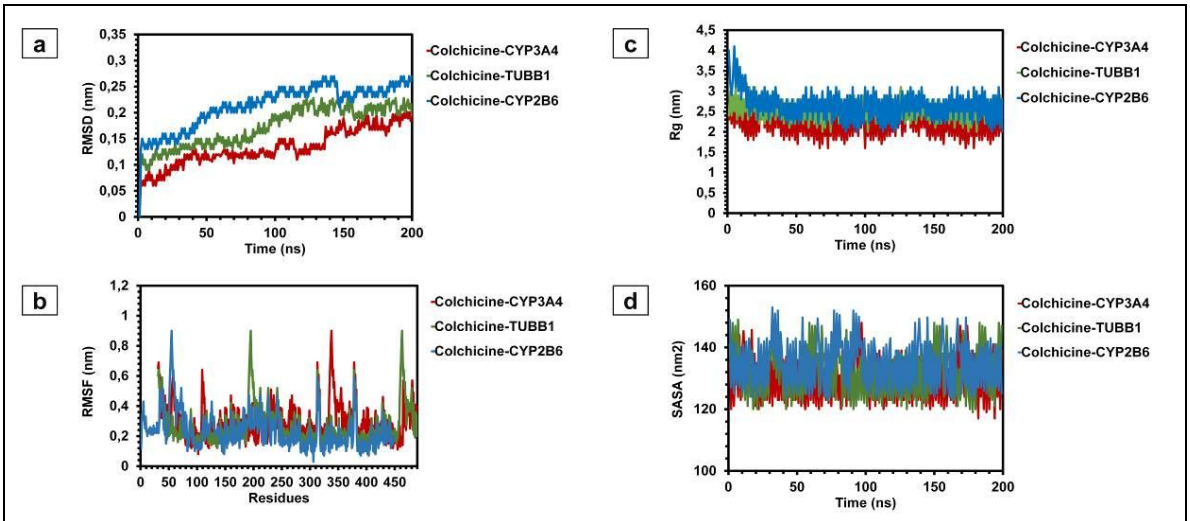


Figure 7. The **(a)** RMSD, (**b)** RMSF, (**c)** Rg, (**d)** SASA values of CYP3A4 (red color), TUBB1 (green color), and CYP2B6 (blue color) during 200 ns MD simulations.

Table 4. The physicochemical and ADMET properties of colchicine.

ADMET properties	Colchicine	
	Value	**Remark**
Physicochemical		
Molecular weight	399.17 g/mol	Proper
A Log P	1.038	Optimal
Hydrogen bond donor	1	Optimal
Hydrogen bond acceptor	6	Optimal
Lipinski rules	Accepted	Accepted
Absorption		
Human intestinal absorption	>30%	Excellent
P-gp-inhibitor	---	Non-inhibitor
P-gp-substrate	++	Substrate
Distribution		
Plasma protein binding	91.2 %	High
Fraction Unbound in plasma	7.6%	Medium
Brain Penetration	---	Excellent
Metabolism		
CYP1A2 inhibitor	---	Non-inhibitor
CYP1A2 substrate	++	Substrate
CYP2C19 inhibitor	---	Non-inhibitor
CYP2C19 substrate	+	Substrate
CYP2C9 inhibitor	---	Non-inhibitor
CYP2C9 substrate	---	Non-substrate
CYP2D6 inhibitor	---	Non-inhibitor
CYP2D6 substrate	---	Non-substrate
Excretion		
Clearance	2.937	Low
Toxicity		
Hepatotoxicity	---	Non-toxic
Carcinogenicity	---	Non-cardiogenic
h-ERG BlOCKERS	---	Inactive

However, colchicine was identified as a P-gp substrate, suggesting transporter-mediated efflux from enterocytes back into the intestinal lumen, which may contribute to reduced intestinal absorption and lower oral bioavailability. Nevertheless, this limitation may be offset by its high predicted human intestinal absorption and lack of inhibition of P-gp.

Based on the distribution profile (Table 4; Annex 2), colchicine showed a plasma protein binding (PPB) value of 91.2%, which is categorized as high (>90%). Elevated PPB values may indicate a narrow therapeutic index and a greater potential for toxicity, due to the drug's extensive binding to plasma proteins, resulting in a lower proportion of free drug available to exert pharmacological effects on target cells.

Conversely, analysis of the fraction of unbound (FU) drug in plasma revealed that colchicine exhibited an FU value of 7.6%, which is classified as moderate (5–20%). This moderate FU value suggested that an adequate proportion of free colchicine remained available in the plasma circulation. These findings suggest a potentially acceptable pharmacokinetic profile, although experimental validation is required.

Based on the excretion profile, colchicine demonstrated a clearance value of 2.97, which was

categorized as low. Furthermore, toxicity prediction indicated that colchicine was non-carcinogenic and exhibited low hepatotoxic and cardiotoxic potentials. In particular, colchicine was predicted not to block the human Ether-à-go-go-Related Gene (hERG), thereby suggesting a low risk of inducing fatal cardiac arrhythmias.

DISCUSSION

Based on previous studies, genetic factors also play a pivotal role in ISR pathogenesis (Asgarbeik et al., 2022). Some mechanisms contributing to ISR include Early elastic return (recoil), neo-atherosclerosis, vascular remodeling, and neointimal hyperplasia (Buccheri et al., 2016). Therefore, these findings provide opportunities to identify ISR-associated therapeutic targets and understand their pathogenesis as novel therapeutic targets, while recognizing that this remains challenging and that the incidence of ISR remains high. On the other hand, identifying the agent that targets the critical gene in the pathogenesis of ISR is also pivotal. Recently, colchicine has been known to have therapeutic effects on some cardiovascular diseases, such as myocardial infarction and cardiac fibrosis (Younas et al., 2025). However, more research on colchicine's specific impact and role in preventive treatment for ISR is needed due to the limited studies on this topic.

Network pharmacology analysis identified the top 3 potential gene targets for colchicine that are also involved in ISR pathogenesis: CYP3A4, TUBB1, and CYP2B6. Some previous studies also revealed that some of these genes have a pivotal role in cardiovascular diseases, including cardiac fibrosis, myocardial infarction, heart failure, and cardiac tissue inflammation (Adu-Amankwaah et al., 2021; Feng et al., 2023; Florek et al., 2024; Han et al., 2020; Wang et al., 2021). Theoretically, CYP3A4 and CYP2B6 belong to the CYP enzyme family and are involved in drug metabolism and elimination, thereby influencing plasma drug concentrations. Increased activity of these enzymes may lead to therapeutic failure by reducing drug concentrations below the therapeutic range (Patel et al., 2026; Zhao et al., 2021). These findings suggest a potential association of these enzymes with ISR-related pathways. In patients with restenosis, altered activity of these enzymes may affect the efficacy of maintenance pharmacotherapy, including antiplatelet agents used to prevent thrombotic events. However, CYP3A4 and CYP2B6 may be more relevant to colchicine metabolism and pharmacokinetic modulation than to direct ISR suppression. Therefore, their prioritization should be interpreted cautiously and validated experimentally. The functional enrichment analysis also revealed significant (FDR $p<0.05$) gene ontology and pathways of the core gene targets, including epoxygenase p40 pathways, arachidonate metabolic process, long chain fatty acid metabolic process, and steroid metabolic process; all of which are pivotal in ISR's pathomechanisms, as well as being processes influenced by colchicine in the preventive treatment of ISR.

Based on binding affinity, TUBB1 showed the most favorable predicted interaction with colchicine (−7.4 kcal/mol), followed by CYP3A4 (−7.1 kcal/mol) and CYP2B6 (−6.9 kcal/mol), which are categorized as moderate binding. This is because the lower the binding affinity, the easier it is for the ligand to bind its target protein. Based on the type of interaction, TUBB1 demonstrated the most favorable docking interaction among the evaluated targets, because colchicine has a large number of interactions with the active sites of TUBB1, especially in the form of hydrogen bonds, which are conventional hydrogen bonds with Gln11, Ser138, Tyr222; carbon hydrogen bond with Ser138, Asp177; and Van der Waals interactions with Gly10, Gly13, Gln15, Gly140, Gly141, Thr143, Gly144, Val169, Ser176, Thr178, Asn204.

MD simulation analysis over 200 ns also revealed that these 3 core targets maintain a stable conformation when bound to colchicine, as indicated by RMSD, RMSF, Rg, and SASA. Fluctuations in RMSD indicated instability in the ligand-target complex, while minimal fluctuations suggested that the system had stabilized. The average value or the fluctuations of RMSD below 2.5 Å are acceptable for a stable ligand-protein interaction. In contrast, fluctuations over 3 Å indicate whether the protein has a significant conformational change during the simulation or is unstable (Patel & Iii, 2004). Based on the RMSD values, CYP3A4 demonstrated the most favorable predicted target among the evaluated proteins, with an average RMSD of 0.132 ± 0.035 nm (1.32 Å), followed by TUBB1 and CYP2B6, with average RMSD values of 0.172 ± 0.039 nm (1.72 Å) and 0.21 ± 0.0417 nm (2.10 Å), respectively. On the other hand, RMSF is used to assess the stability and mobility of local proteins upon ligand binding to the target. High RMSF values are predicted to indicate weaker interactions and stability between the ligands and the receptor (Martínez, 2015). The results show that the lowest average RMSF value for core targets in the complex with colchicine is CYP2B6, with an average RMSF of 0.23 nm (2.3 Å). The Rg was used as an indicator of structural stability and compactness; the CYP3A4 complex exhibited the most stable conformation, followed by TUBB1 and CYP2B6, based on Rg analysis. SASA was employed to describe protein–solvent interactions, reflecting the extent of conformational changes during ligand binding and serving as an indicator of protein accessibility. Overall, the CYP3A4 complex showed the lowest SASA values, indicating a more compact and stable interaction with colchicine,

followed by TUBB1 and CYP2B6. Furthermore, based on MM-GBSA analysis, the colchicine–TUBB1 complex exhibited the most favorable predicted binding free energy with a binding free energy of −54.17 ± 5.86 kcal/mol, followed by CYP3A4 and CYP2B6 complexes. Together, these findings suggest that colchicine may interact with selected ISR-associated proteins *in silico*. However, these results should be interpreted as hypothesis-generating because direct target engagement, pathway modulation, and anti-restenotic activity have not yet been experimentally confirmed.

In summary, this study identified potential colchicine-associated targets and signaling pathways relevant to ISR using gene network-based pharmacology analysis, molecular docking, and MD simulations. However, this study still has some limitations. Firstly, the ISR-related genes were compiled from public databases, involving 8,438 putative ISR-associated genes. This extensive set is sufficiently broad to introduce the possibility of database noise and target inflation. To minimize this limitation, multiple filtering and prioritization steps, including network topology analysis, molecular docking, and molecular dynamics simulations, were applied. Secondly, because a single MD trajectory was performed for each complex, stochastic variability in ligand–protein behavior could not be fully assessed. Replicate simulations are recommended in future work to improve statistical robustness. Lastly, the gene network-based pharmacology analysis, molecular docking, and MD simulations are based on database screening and computational predictions. Therefore, further validation through in vitro studies is required, such as VSMC proliferation and migration assays, endothelial migration or tube-formation assays, inflammatory cytokine assays (IL-1β, IL-6, TNF-α), and target pathway validation via Western blot or qPCR. In vivo and clinical studies are also needed to confirm the activity and appropriate dose of colchicine for the treatment of ISR.

CONCLUSION

Network pharmacology, molecular docking, molecular dynamics simulation, and MM-GBSA analyses were applied to identify potential colchicine-associated targets in ISR. CYP3A4, TUBB1, and CYP2B6 were prioritized as candidate proteins, with TUBB1 showing the most favorable predicted interaction among the evaluated targets. These findings provide computational evidence for potential colchicine–target interactions in ISR-related pathways, but experimental validation is required before biological or clinical conclusions can be drawn.

CONFLICT OF INTEREST

The research was conducted entirely free from any involvement in commercial, financial, or personal matters that might be perceived as a possible conflict of interest or that could have influenced the outcomes or interpretation of the study.

ACKNOWLEDGMENTS

This research did not receive any specific grant from funding agencies in the public, commercial, or not-for-profit sectors.

GENERATIVE ARTIFICIAL INTELLIGENCE (AI)

The authors used Grammarly Pro and ChatGPT Plus to improve the language and readability of the manuscript. The authors reviewed and edited the content and take full responsibility for its accuracy. No images were generated or manipulated using AI tools.

REFERENCES

Adu-Amankwaah J, Adzika GK, Adekunle AO, Ndzie Noah ML, Mprah R, Bushi A, Akhter N, Huang F, Xu Y, Adzraku SY, Nadeem I, Sun H (2021) ADAM17, a key player of cardiac inflammation and fibrosis in heart failure development during chronic catecholamine stress. Front Cell Dev Biol 9: 732952. https://doi.org/10.3389/fcell.2021.732952

Alfonso F, Coughlan JJ, Giacoppo D, Kastrati A, Byrne RA (2022) Management of in-stent restenosis. EuroIntervention 18: E103–E123. https://doi.org/10.4244/EIJ-D-21-01034

Amien MI, Nurhidayat BR, Rizqa SU, Arfiani SZ, Widiastuti LN, Isbach GP (2026) Computational design of a novel chimeric multi-epitope vaccine against chlamydia trachomatis serovar a to prevent trachoma. Braz J Microbiol 57: 160. https://doi.org/10.1007/s42770-026-01977-x

Asgarbeik S, Vahidi A, Hasanzad M, Asadi M, Amoli MM (2022) Vascular endothelial growth factor genetic variant is associated with in-stent restenosis after percutaneous coronary intervention. J Tehran Univ Heart Cent 17: 119–126. https://doi.org/10.18502/jthc.v17i3.10844

Buccheri D, Piraino D, Andolina G, Cortese B (2016) Understanding and managing in-stent restenosis: a review of clinical data, from pathogenesis to treatment. J Thorac Dis 8: E1150–E1162. https://doi.org/10.21037/jtd.2016.10.93

Cao X, Zao X, Xue B, Chen H, Zhang J, Li S, Li X, Zhu S, Guo R, Li X, Ye Y (2021) The mechanism of TiaoGanYiPi formula for treating chronic hepatitis B by network pharmacology and molecular docking verification. Sci Rep 11: 8402. https://doi.org/10.1038/s41598-021-87812-9

Case DA, Aktulga HM, Belfon K, Cerutti DS, Cisneros GA, Cruzeiro VWD, Forouzesh N, Giese TJ, Götz AW, Gohlke H, Izadi S, Kasavajhala K, Kaymak MC, King E, Kurtzman T, Lee TS, Li P, Liu J, Luchko T, Merz KM (2023) AmberTools. J Chem Inf Model 63: 6183–6191. https://doi.org/10.1021/acs.jcim.3c01153

Cassese S, Byrne RA, Schulz S, Hoppman P, Kreutzer J, Feuchtenberger A, Ibrahim T, Ott I, Fusaro M, Schunkert H, Laugwitz KL, Kastrati A (2015) Prognostic role of restenosis in 10 004 patients undergoing routine control angiography after coronary stenting. Eur Heart J 36: 94–99. https://doi.org/10.1093/eurheartj/ehu383

Curcio A, Torella D, Indolfi C (2011) Mechanisms of smooth muscle cell proliferation and endothelial regeneration after vascular

injury and stenting: Approach to therapy. Circ J 75: 1287–1296. https://doi.org/10.1253/circj.CJ-11-0366

Feng A, Caro YM, Gardner C, Grischo G, Liang Y, Wickremasinghe PD, Polmann M, Kala M, Marlowe T, Black SM, Knox KS, Wang T (2023) PTK2-associated gene signature could predict the prognosis of IPF. Respir Res 24: 304. https://doi.org/10.1186/s12931-023-02582-4

Florek K, Mendyka D, Gomułka K (2024) Vascular endothelial growth factor (VEGF) and its role in the cardiovascular system. Biomedicines 12: 1055. https://doi.org/10.3390/biomedicines12051055

Han Z, Wu X, Gao Y, Liu X, Bai J, Gu R, Lan RF, Xu B, Xu W (2020) PDK1–AKT signaling pathway regulates the expression and function of cardiac hyperpolarization-activated cyclic nucleotide-modulated channels. Life Sci 250: 117546. https://doi.org/10.1016/j.lfs.2020.117546

Hijazi M, Wilkins DM, Ceriotti M (2018) Fast-forward Langevin dynamics with momentum flips. J Chem Phys 148: 184109. https://doi.org/10.1063/1.5029833

Jo S, Kim T, Iyer VG, Im W (2008) CHARMM-GUI: A web-based graphical user interface for CHARMM. J Comput Chem 29: 1859–1865. https://doi.org/10.1002/jcc.20945

Kim S, Chen J, Cheng T, Gindulyte A, He J, He S, Li Q, Shoemaker BA, Thiessen PA, Yu B, Zaslavsky L, Zhang J, Bolton EE (2023) PubChem 2023 update. Nucleic Acids Res 51: D1373–D1380. https://doi.org/10.1093/nar/gkac956

Martínez L (2015) Automatic identification of mobile and rigid substructures in molecular dynamics simulations and fractional structural fluctuation analysis. PloS ONE 10: e0119264. https://doi.org/10.1371/journal.pone.0119264

Park DW, Hong MK, Mintz GS, Lee CW, Song JM, Han KH, Kang DH, Cheong SS, Song JK, Kim JJ, Weissman NJ, Park SW, Park SJ (2006) Two-year follow-up of the quantitative angiographic and volumetric intravascular ultrasound analysis after nonpolymeric paclitaxel-eluting stent implantation: Late "catch-up" phenomenon from ASPECT study. J Am Coll Cardiol 48: 2432–2439. https://doi.org/10.1016/j.jacc.2006.08.033

Patel S, Brooks CL III (2004) CHARMM fluctuating charge force field for proteins: I parameterization and application to bulk organic liquid simulations. J Comput Chem 25: 1–15. https://doi.org/10.1002/jcc.10355

Patel T, Rahimi N, Cassagnol M (2026) Biochemistry, Cytochrome P450. In: StatPearls [Internet]. StatPearls Publishing, Treasure Island (FL). https://www.ncbi.nlm.nih.gov/books/NBK557698/

Phillips JC, Hardy DJ, Maia JDC, Stone JE, Ribeiro JV, Bernardi RC, Buch R, Fiorin G, Hénin J, Jiang W, McGreevy R, Melo MCR, Radak BK, Skeel RD, Singharoy A, Wang Y, Roux B, Aksimentiev A, Luthey-Schulten Z, Tajkhorshid E (2020) Scalable molecular dynamics on CPU and GPU architectures with NAMD. J Chem Phys 153: 044130. https://doi.org/10.1063/5.0014475

Suryono S, Amien MI, Tohari AI, Saputra AD, Hidayat MR, Ramadhan HF (2025) *In silico* studies on quercetin, myricetin, and kaempferol in inhibiting TGF-β1 and galectin-3 for cardiac fibrosis management. Narra J 5: e1310. https://doi.org/10.52225/narra.v5i1.1310

Suryono S, Rohman MS, Widjajanto E, Prayitnaningsih S, Wihastuti TA, Oktaviono YH (2023) Effect of colchicine in reducing MMP-9, NOX2, and TGF-β1 after myocardial infarction. BMC Cardiovasc Disord 23: 449. https://doi.org/10.1186/s12872-023-03464-9

Trott O, Olson AJ (2010) AutoDock Vina: Improving the speed and accuracy of docking with a new scoring function, efficient optimization, and multithreading. J Comput Chem 31: 455–461. https://doi.org/10.1002/jcc.21334

Verschuren JJW, Trompet S, Postmus I, Sampietro ML, Heijmans BT, Houwing-Duistermaat JJ, Slagboom PE, Jukema JW (2012) Systematic testing of literature reported genetic variation associated with coronary restenosis: Results of the GENDER study. PLoS One 7: e42401. https://doi.org/10.1371/journal.pone.0042401

Wang Z, Zhao YT, Zhao TC (2021) Histone deacetylases in modulating cardiac disease and their clinical translational and therapeutic implications. Exp Biol Med 246: 213–225. https://doi.org/10.1177/1535370220944128

Younas A, Awan Z, Khan T, Mehta S, Munir A, Raja HAA, Jain H, Raza A, Sehar A, Ahmed R, Nashwan AJ (2025) The effect of colchicine on myocardial infarction: An updated systematic review and meta-analysis of randomized controlled trials. Curr Probl Cardiol 50: 102878. https://doi.org/10.1016/j.cpcardiol.2024.102878

Zhang DM, Chen S (2020) In-stent restenosis and a drug-coated balloon: Insights from a clinical therapeutic strategy on coronary artery diseases. Cardiol Res Pract 2020: 8104939. https://doi.org/10.1155/2020/8104939

Zhao M, Ma J, Li M, Zhang Y, Jiang B, Zhao X, Huai C, Shen L, Zhang N, He L, Qin S (2021) Cytochrome P450 enzymes and drug metabolism in humans. Int J Mol Sci 22: 12808. https://doi.org/10.3390/ijms222312808

AUTHOR CONTRIBUTION:

Contribution	Suryono S	Amien MI	Tohari AI	Saputra AD	Hidayat MRF	Hibatullah MN	Ramadhan HF	Hibatulloh MF
Concepts or ideas	x	x	x	x	x	x	x	x
Design	x	x	x	x	x	x	x	x
Definition of intellectual content	x							
Literature search	x	x	x			x		
Data acquisition	x	x	x	x	x	x	x	x
Data analysis		x	x			x		
Statistical analysis		x	x			x		
Manuscript preparation	x	x	x	x	x	x	x	x
Manuscript editing	x	x	x	x	x	x	x	x
Manuscript review	x	x	x	x	x	x	x	x

Citation Format: Suryono S, Amien MI, Tohari AI, Saputra AD, Hidayat MRF, Hibatullah MN, Ramadhan HF, Hibatulloh MF (2026) Integrated network pharmacology and molecular simulation analysis of colchicine in coronary in-stent restenosis. J Pharm Pharmacogn Res 14(4): 2545. https://doi.org/10.56499/jppres_14.4.2545

Publisher's Note: All claims expressed in this article are solely those of the authors and do not necessarily represent those of their affiliated organizations, or those of the publisher, the editors and the reviewers. Any product that may be evaluated in this article, or claim that may be made by its manufacturer, is not guaranteed or endorsed by the publisher.

Open Access: This article is distributed under the terms of the Creative Commons Attribution 4.0 International License (http://creativecommons.org/ licenses/by/4.0/), which permits use, duplication, adaptation, distribution and reproduction in any medium or format, as long as you give appropriate credit to the original author(s) and the source, provide a link to the Creative Commons license and indicate if changes were made.

Supplementary data

Annex 1. Redocking validation

https://drive.google.com/file/d/18YL8-wB7XeSC6hq8_iDjJOk3AIrceHQH/view?usp=sharing

Annex 2. ADMET

https://drive.google.com/file/d/1JvjGQ9ImbZQCF5lHUZb8L8z9nfmPDnRu/view?usp=sharing

Table S1. Identification of ISR-related genes.

https://docs.google.com/spreadsheets/d/1MMkYevzIbX_ILaOUZsNBKeDpFhxqNS3-/edit?usp=sharing&ouid=106353289139040512845&rtpof=true&sd=true

Table S2. Putative gene targets of colchicine.

https://docs.google.com/spreadsheets/d/1raHsQzNqLR0gln7srInHDqueh9b1VZvU/edit?usp=sharing&ouid=103334443576438792849&rtpof=true&sd=true

Table S3. Potential colchicine-ISR common targets.

https://docs.google.com/spreadsheets/d/1P308pyJMIPaVDvUmmm0CfKEXVmFDdF33/edit?usp=sharing&ouid=106353289139040512845&rtpof=true&sd=true